

# Polarization of Secondary Electrons from Clean and Oxygen-Chemisorbed Ni(110)

Y. Oshima, T. Yamada, J. Fujii, and T. Mizoguchi

Faculty of Science, Gakushuin University  
1-5-1 Mejiro, Toshima-ku, Tokyo 171-8588, Japan

The saturation spin polarization of secondary electrons from a clean Ni(110) surface was quantitatively measured at 0.094 after careful calibration of a compact Mott detector installed in an Auger electron analyzer for strict inspection of the cleanness of the surface. The spin-dependent mean absorption length of Ni(110) was deduced to be about four layers of Ni(110), that is,  $\lambda_{+} = 1.016$  nm and  $\lambda_{-} = 0.972$  nm for the majority spin and minority spin electrons, respectively, from the primary electron energy dependence of the yield and the asymmetry of secondary electrons. The saturation spin polarization was reduced to 0.060, that is, 64% of that for the clean Ni(110) surface, after only 1 hour in a UHV chamber ( $2 \times 10^{-7}$  Pa) following a cleaning procedure, for sub-mono-layer oxygen-chemisorbed Ni(110). A model of anti-ferromagnetic Ni spin moments resulting from 180-degree super-exchange through oxygen atoms in the first layer, based on reported STM observations of Ni-O atomic arrangement, is proposed for use in further investigations to explain this drastic reduction in the polarization, which must be very sensitive to the surface magnetic configuration.

**Key words:** spin polarization of secondary electrons, oxygen-chemisorbed, spin-dependent mean absorption length, anti-ferromagnetic, 180-degree super-exchange

## 1. Introduction

Since the first demonstration that secondary electrons from ferromagnetic materials are spin-polarized <sup>1)</sup>, several detailed studies have been reported. The energy-resolved spin polarization of secondary electrons from Ni(110) shows structures in the spin-polarization spectrum <sup>2)</sup>. Theory tells us that the ratio of lifetimes of electrons with majority- to minority-spin can be determined directly from the measured value of the spin polarization and the bulk magnetization <sup>3)</sup>. The spin polarization of low-energy secondary electrons has a strong surface sensitivity, suggesting a mean magnetic probing depth of only three to four atomic layers, contrary to estimates based on the universal escape-depth curve <sup>4)</sup>.

Koike and Kirschner proposed a model for the primary electron energy dependence of secondary electron polarization and deduced the spin-dependent net mean absorption lengths of secondary electrons, namely,  $\lambda_{+} = 0.850$  nm and  $\lambda_{-} = 0.750$  nm, for the

majority-spin and minority-spin electrons, respectively, in a permalloy (Ni<sub>78.5</sub>Fe<sub>21.5</sub>) poly-crystal <sup>5)</sup>. The polarization is determined primarily by the polarization of electrons created directly by primary electrons, but is also enhanced by the mutually different spin-dependent absorption lengths for majority and minority spins.

The observation of magnetic domain by means of a scanning electron microscope with spin polarization analyzer (SEMPA) is impressive but rather easy, because it is sufficient to make a qualitative contrast. On the other hand, for the quantitative measurement of the spin polarization of secondary electrons in basic research on surface magnetism, a spin-polarization detector (polarimeter) must be carefully calibrated.

Since the spin polarization of secondary electrons from ferromagnetic metals is quite sensitive to surface contamination, it is crucial to prepare a very clean homogeneous single magnetic domain surface in order to investigate the intrinsic magnetic properties of the surface. Observation of the cleanness of surface by Auger spectroscopy must be performed simultaneously with spin-polarization measurement.

It is also important to avoid any stray field from a ferromagnetic sample, because low-energy secondary electrons are easily affected by a magnetic field.

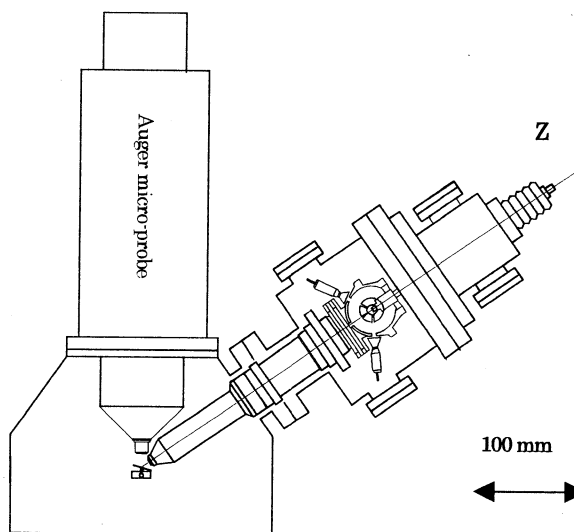


**Fig. 1** Home-made compact Mott polarimeter installed in an auxiliary port of an Auger electron microprobe analyzer (JEOL, JAMP30).

## 2. Experimental

A typical ferromagnetic metal, pure single-crystal Ni(110), was shaped in a skewed picture frame to create a closed magnetic flux, thus avoiding any stray field from the sample. This sample had been cleaned frequently in UHV for nearly a decade in our laboratory to reduce contamination.

In order to measure the polarization of secondary electrons from ferromagnetic materials, three versions of Mott detectors with acceleration voltages of 150 eV<sup>6</sup>, 7), 60 keV<sup>8</sup>, 15 keV, respectively, were used. The first and third were constructed in our laboratory, while the second one was manufactured by Mitsubishi Heavy Industries Ltd. The third one was installed in an auxiliary port of an Auger electron analyzer (JEOL-JAMP30), as shown in Fig. 1. The primary electron beam current for the polarization measurement was typically 100 nA for the scanning electron microscopy (SEM) mode and for Auger analysis mode, 500 nA for the polarization measurements.

The secondary electrons from a sample surface were accelerated by a typical operating voltage, 15 kV, to hit an Au target. The scattered electrons from the Au target were decelerated in a spherical potential between the inner and outer spherical electrodes. Four or up to eight channeltrons were installed to detect asymmetric scattering of polarized electrons with the scattering angle of 120° at various azimuths  $\phi = n\pi/4$  ( $n = 0$  to 7) around the Z axis. The X and Y axis in Fig. 3 are defined in the directions of  $\phi = 0$  and  $\phi = \pi/2$ , respectively.

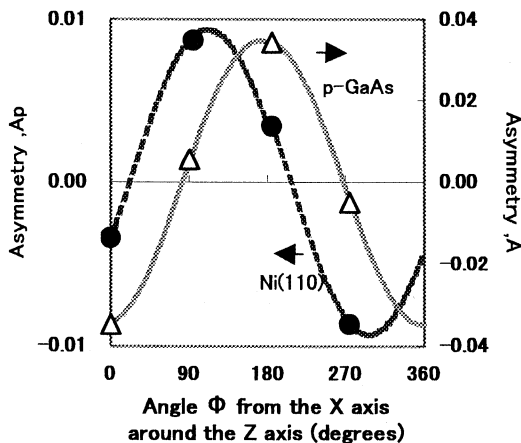


**Fig. 2** Asymmetry of scattered electrons from an Au target in the Mott detector for a polarized electron beam from a p-GaAs source ( $\Delta$ ) and secondary electrons from Ni(110) ( $\bullet$ ) as a function of the azimuth angle  $\phi = n \times 90^\circ$  ( $n = 0$  to 3) from the X axis around the Z axis. The peak position of the latter is  $108^\circ$ , indicating that the direction of magnetization is  $18^\circ$  from the X axis.

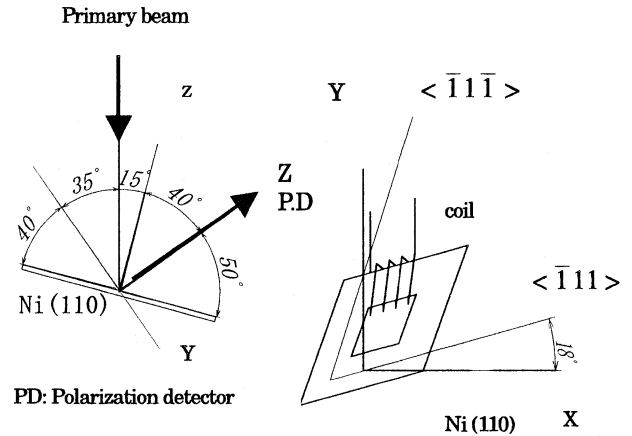


**Fig.3** Angle between the normal of the Ni(110) sample (z axis) and a primary electron beam and the direction of the polarimeter (Z axis) (left). Shape of a picture-frame Ni single-crystal sample with legs in the easy direction for magnetization (right).

The inputs of channeltrons were kept at ground level in the polarization measurement, in which all secondary electrons with kinetic energies from 0 to about 30 eV were counted.

The polarimeter was calibrated by using a polarized electron beam with 30% polarization ( $P = 0.30$ ) from a p-GaAs source illuminated with circularly polarized light of 1.52 eV<sup>9</sup>. The ratio of the difference to the sum of the counting rates of each channeltron for up or down polarized photo-electrons obtained by right- and left- circularly polarized light illumination is plotted in Fig. 2 with the various azimuths  $\phi = n\pi/4$  ( $n = 0, 2, 4, 6$ ) where the four channeltrons were located. The asymmetry  $A_P$  of the left and right scattering is obtained by Fourier fitting of these plots. In a typical polarization measurement, we have the Sherman function,  $S = A_P/P = 0.12$  and the quality factor,  $Q = S^2 (I/I_0) = 2 \times 10^{-6}$ .

The incident angle of the primary electron beam was  $15^\circ$  from the normal of the Ni(110) sample surface, as shown in Fig. 3. The secondary electrons were guided to the polarimeter along the Z axis at an angle of  $40^\circ$  from the normal of the sample surface. The sample was shaped in a skewed picture frame composed of  $\langle 111 \rangle$  and  $\langle 1\bar{1}1 \rangle$  legs, both of which were in the easy direction of a Ni single crystal. The current coil was wound around one of the legs to control magnetization direction. The ratios of the difference to the sum of the counting rates of the four channeltrons for mutually opposite magnetization directions are also plotted in Fig. 2. The amplitude of Fourier fitting of the plot indicates the polarization of secondary electrons from the sample, and the phase indicates that the direction of the magnetization is  $18^\circ$  from the X axis, as shown in Fig. 3.

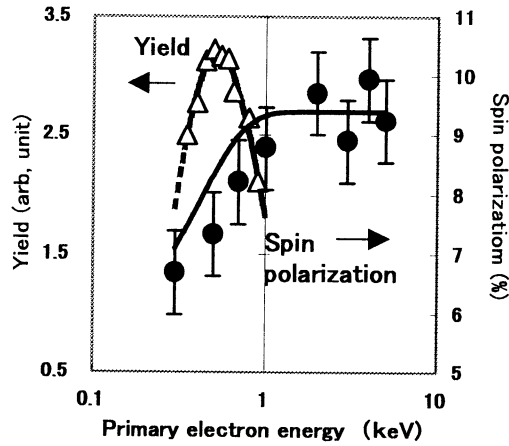


**Fig. 4** Yield ( $\Delta$ ) and polarization ( $\bullet$ ) of secondary electrons from Ni(110) as a function of the primary electron energy.

In order to prepare a clean surface, the sample was heated up to 550 °C for 20 min, sputter-etched with Ar ion and finally annealed at 550 °C for 5 min. The vacuum level of the measurement chamber was kept at less than  $2 \times 10^{-7}$  Pa. All measurements were performed at room temperature.

### 3. Results and Discussion

The polarization of secondary electrons from a clean Ni (110) surface increased with the primary electron energy ( $E_p$ ) and saturated at a value of 0.094 for  $E_p > 1$  keV, while the observed secondary electron yield showed a maximum at a primary electron energy of 0.5 keV, as shown in Fig. 4.

First we derive the mean net absorption length of the secondary electrons in Ni metal from the primary energy dependence of the secondary electron yield<sup>5)</sup>. The penetration range  $R$  (in keV) in Ni metal of a primary electron of energy  $E_p$  (in keV) is obtained as

$$R = 6.2 \times 10^{-7} E_p^{\frac{4}{3}} \quad (1)$$

by inserting the atomic density,  $9.17 \times 10^{22} \text{ cm}^{-3}$  and atomic number, 28, for Ni into the semi-empirical formula<sup>10-12)</sup>.

The secondary electrons are created within a layer of thickness

$$R_z = R \cos \theta \quad (2)$$

below the surface by primary electrons with an incident angle  $\theta = 15^\circ$  from the normal of the sample surface. The number of secondary electrons  $ndz$  produced in a layer of thickness  $dz$  at a depth of  $z$  ( $0 \leq z \leq R_z$ ) below the surface can then be expressed as a step function<sup>5,13,14)</sup>,

$$ndz = \frac{E_p}{E_d R_z} dz, (0 \leq z \leq R_z) \quad (3)$$

where  $E_d$  is the average energy needed to create the secondary electrons.

Using a net mean absorption length  $\lambda$  of secondary electrons, including the cascade process and the escape probability  $B$  at the surface, the yield of secondary electrons emitted from the surface is obtained as

$$y = \int_0^{R_z} nB \exp\left(-\frac{z}{\lambda}\right) dz \quad (4)$$

$$= B \frac{E_p \lambda}{E_d R_z} \left[ 1 - \exp\left(-\frac{R_z}{\lambda}\right) \right]$$

The observed secondary electron yield shows a maximum at  $E_p = 0.5$  keV, at which the Eqs. (1) and (2) give  $R_z = 2.47$  nm. By fitting Eq. (4), where  $R_z$  depends on  $E_p$ , to the observed data, the net mean absorption length is found to be  $\lambda = 0.994$  nm and  $B/E_d = 14.5$  (keV)<sup>-1</sup> for a clean Ni(110) surface. This means that only four (0.994/0.249) Ni(110) layers contribute significantly to the emission of secondary electrons. This should be recognized in order to understand how the polarization of secondary electrons is sensitive to a few layers from the surface of a magnetic sample. Taking  $E_d$  as a few eV we get the escape probability  $B$  of the secondary electrons from a surface as in the order of  $10^{-2}$ .

The polarization of secondary electrons from a ferromagnetic metal is not simply the polarization  $P_0$  of conduction electrons in a metal, but is affected by mutually different spin-dependent absorption lengths,  $\lambda_+$  and  $\lambda_-$  for majority and minority spin electrons, respectively. By introducing spin-dependent net mean absorption lengths, the spin-dependent secondary electron yields  $y_+$  and  $y_-$  can be given as follows:

$$y_{\pm} = \frac{1 \pm P_0}{2} \frac{E_p B}{R_z E_d} \lambda_{\pm} \left[ 1 - \exp\left(-\frac{R_z}{\lambda_{\pm}}\right) \right] \quad (5)$$

The spin polarization of secondary electrons is then given as

$$P = \frac{y_+ - y_-}{y_+ + y_-} \quad (6)$$

The spin-dependent mean absorption lengths are expressed as

$$\lambda_{\pm} = \lambda (1 \pm A_{\lambda}) \quad (7)$$

by using the asymmetry

$$A_{\lambda} = \frac{\lambda_+ - \lambda_-}{\lambda_+ + \lambda_-} \quad (8)$$

From Eq. (5) the saturation polarization  $P_s$  at  $E_p \rightarrow \infty$  is given as

$$P_s = \lim_{E_p \rightarrow \infty} \frac{y_+ - y_-}{y_+ + y_-} = \frac{A_\lambda + P_0}{1 + P_0 A_\lambda} \quad (9)$$

The saturation polarization of secondary electrons for  $E_p > 1$  keV is found to be  $P_s = 0.094$  for clean Ni(110). Taking the polarization  $P_0$  of Ni conduction band as 0.050<sup>5)</sup>, the asymmetry of the mean absorption length is obtained as  $A_\lambda = 0.044$ . The spin-dependent absorption length then turns out to be  $\lambda_+ = 1.016$  nm and  $\lambda_- = 0.972$  nm for a clean Ni(110) surface.

The saturation polarization  $P_s$  of secondary electrons from the Ni sample decreases with time from 0.094 to 0.060 (a 64% reduction) within about one hour of the surface cleaning procedure, as shown in Fig. 5. In Fig. 6 the Auger spectra of the sample measured just after the cleaning treatment and 2 hours after the cleaning in an Auger spectrometer chamber ( $2 \times 10^{-7}$  Pa) at room temperature are shown. A clear increase of oxygen Auger electron peak amplitude at 512 eV occurs during these 2 hours. The time dependence of the Auger peak-to-peak height ratio of O/Ni is shown in Fig. 5, where the O/Ni ratio becomes almost constant (roughly 1/4), suggesting that rather stable oxygen-chemisorbed surface reconstruction occurs on Ni(110). No increase of carbon peak is detected in Auger spectra.

It is clear that the polarization of the secondary electrons is quite sensitive to the magnetic state of the surface of a sample, because only about four layers are responsible for the emitted secondary electrons.

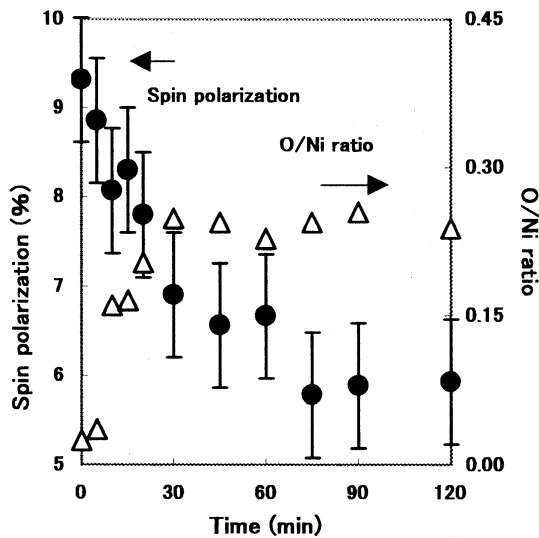


**Fig. 5** Polarization of the secondary electrons (●) and O/Ni Auger peak-to-peak ratio (△) of a Ni(110) sample with time in a Auger electron analyzer chamber of  $2 \times 10^{-7}$  Pa after the cleaning procedure.

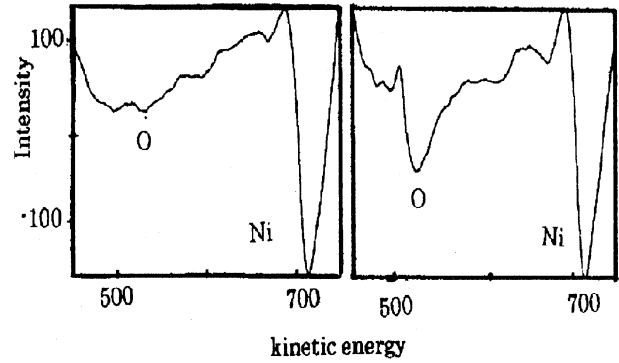


**Fig. 6** Auger spectrum of a clean Ni(110) surface just after cleaning (left) and 2 hours after cleaning (right) in a Auger electron analyzer chamber of  $2 \times 10^{-7}$  Pa.

The polarization is sensitive to the depth direction, but the lateral resolution depends on the primary electron beam diameter, which is rather broad (100 nm), since a high beam current is necessary for polarization analysis. For lateral information LEED or STM must be effective.

Several STM investigations of oxygen-chemisorbed Ni(110) have been reported<sup>15-19)</sup>. STM with a good tungsten tip has atomic-scale lateral resolution, but gives no magnetic information of the surface. In some conditions a  $(2 \times 1)$  ordered arrangement of oxygen and Ni formed on the Ni(110) surface, to which the observed O/Ni ratio (roughly 1/4) of Auger peak-to-peak signals may correspond, since Auger electrons come from a few layers of the sample surface. Combining one of the lateral atomic structures obtained by STM with our experimental results, we propose the model of the surface magnetic structure shown in Fig. 7.

When a Ni(110) surface is chemisorbed with oxygen from a sub-mono-layer, the first layer of the (110) plane is composed of Ni-O chains along  $\langle \bar{1}10 \rangle$ . It is well known that the 180-degree super-exchange interaction through oxygen is negative<sup>20-23)</sup>, as can be seen in many transition metal oxides. We therefore consider that there is super-exchange interaction between the spin-magnetic moments of Ni atoms separated by an oxygen atom, which causes anti-ferromagnetic coupling in the first surface layer. This spin configuration in the first layer explains the drastic reduction in the polarization of secondary electrons from an oxygen-chemisorbed surface of Ni(110).

The spin-magnetic moment of Ni in the second (110) layer, which is sandwiched by the anti-ferromagnetic first layer and ferromagnetic bulk, may deviate from the  $\langle \bar{1}11 \rangle$  direction of ferromagnetic bulk magnetization and may also contribute to the reduction in the polarization of secondary electrons.

It would be worthwhile to check this proposed model in future by using a spin-polarized STM, or more easily by conducting spin-polarized LEED experiments, in which the  $4 \times 1$  superlattice spots of magnetic origin would appear.

Both the reduction in the polarization  $P_0$  of the conduction electrons in the effective four layers in Ni(110) surface and the reduction of the asymmetry  $A_\lambda$  of the spin-dependent mean absorption cause a reduction in the spin polarization of the secondary electrons emitted from a sub-mono-layer oxygen-chemisorbed Ni(110) surface. They must satisfy the relation  $P_0 + A_\lambda = 0.060$ , since the denominator in Eq. (9) is almost 1. The polarization of conduction electrons may be reduced to 0.043 by factor 12/14, because 2 Ni atoms in a unit cell in the first layer among 14 Ni atoms in the next four layers from the surface are considered to couple in an anti-parallel manner. The asymmetry of the spin-dependent absorption length thus becomes 0.017. If there are deviation of the second layer Ni moments as shown in Fig. 7 the further reduction of the polarization of conduction electrons would occur.

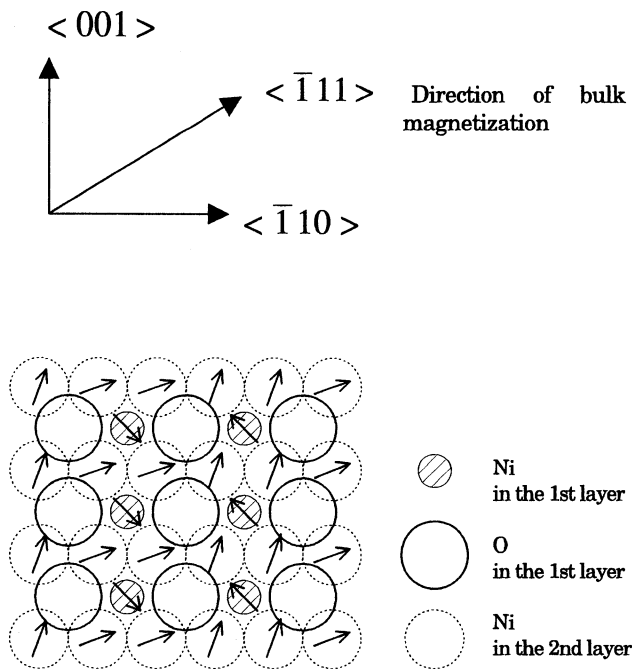


**Fig. 7** Proposed model surface magnetic configuration based on a reported Ni-O  $2 \times 1$  order atomic image obtained by STM. The anti-ferromagnetic Ni spin moments caused by 180 degree super-exchange through oxygen in the first layer and some deviation of the spin direction in the second layer from the bulk magnetization direction are shown schematically by arrows.

## 4. Conclusion

The saturation spin polarization is 0.094 for a clean Ni(110) surface and is reduced to 0.06 for sub-mono-layer oxygen-chemisorbed Ni(110). The spin-dependent mean absorption length of Ni(110) was measured at  $\lambda_+ = 1.016$  nm and  $\lambda_- = 0.972$  nm for majority spin electrons and minority spin electrons, respectively. This very short absorption length (only about four (110) layers in Ni) of secondary electrons explains why the spin polarization of secondary electrons is very sensitive to the magnetic configuration in the surface layers.

It has been shown that it is crucial to prepare a clean and homogeneous intrinsic surface for reliable polarization measurement of a ferromagnetic metal surface. Combination of the polarization analysis with surface analysis, such as Auger spectroscopy, has proved to be quite effective.

A model of anti-ferromagnetic Ni formed by 180-degree super-exchange through oxygen in the first layer, based on reported STM observations of Ni-O atomic arrangement, is proposed for future investigations.

## Acknowledgements

We are grateful to Dr. K. Koike and Prof. H. van Kempen for critical reading of our manuscript. We appreciate Dr. Tsuno's help in designing an electron path in a secondary electron guide.

## References

- 1) G. Chrobok and M. Hofmann: *Phys. Lett.*, 57A, 257 (1976).
- 2) H. Hopster, R. Raue, E. Kisker, G. Guntherodt, and M. Campagna: *Phys. Rev. Lett.*, 50, 70 (1983).
- 3) D. R. Penn: *Phys. Rev. Lett.*, 55, 518 (1985).
- 4) D. L. Abraham and H. Hopster: *Phys. Rev. Lett.*, 58, 1352 (1987).
- 5) K. Koike and J. Kirschner: *J. Phys. D: Appl. Phys.*, 25 1139 (1992).
- 6) J. Unguris, D. T. Pierce, and R. J. Celotta: *Rev. Sci. Inst.*, 57, 1314 (1986).
- 7) M. R. Scheinfein, D. T. Pierce, J. Unguris, J. J. McClelland, R. J. Celotta, and M. H. Kelley: *Rev. Sci. Inst.*, 60, 1 (1989).
- 8) Feder: *Polarized Electrons in Surface Physics*. 5.2.2 Mott detectors., P265-271.
- 9) D. T. Pierce and E. Meier: *Phys. Rev.*, B13, 5484 (1976).
- 10) S. A. Schwarz: *J. Appl. Phys.*, 68, 2382 (1990).
- 11) J. R. Young: *Phys. Rev.*, 103, 292 (1956).
- 12) A. Dekker: *J. Secondary Electron Emission Solid State Phys.*, vol. 6 (New York: Academic), pp. 251-311 (1985).
- 13) F. Dionne: *J. Appl. Phys.*, 44, 5362 (1973).
- 14) J. R. Young: *J. Appl. Phys.*, 28, 524 (1957).
- 15) L. Eierdal: *Surf. Sci.*, 312, 31 (1994).
- 16) F. Besenbacher, I. Stensgaard, L. Ruan, J. K. Nørskov, and K. W. Jacobsen: *Surf. Sci.*, 272, 334 (1992).

- 17) G. Kleinle, J. Wintterlin, G. Ertl, R. J. Behm, F. Jona, and W. Moritz: *Surf. Sci.*, 225,171 (1990).
- 18) B. Voigtlander, S. Lehwald, and H. Ibach: *Surf. Sci.*, 225, 162 (1990).
- 19) L. Ruan, F. Besenbacher, I. Stensgaard, and E. Laegsgaard: *Phys. Rev. Lett.*, 70, 4079 (1993).
- 20) P. W. Anderson: *Phys. Rev.*, 79, 350 (1950).
- 21) J. B. Goodenough: *Phys. Rev.*, 100, 564 (1955).
- 22) J. Kanamori: *J. Phys. Chem. Solids.*, 10, 87 (1959).
- 23) E. O. Wollan, H. R. Child, W. C. Koehler, and M. K. Wilkinson: *Phys. Rev.*, 112,1132 (1958).

( Received July 3, 2001; Accepted September 14, 2001. )